Environmental Science Nano

ROYAL SOCIETY OF CHEMISTRY

PAPER

View Article Online
View Journal | View Issue

Cite this: *Environ. Sci.: Nano*, 2025, **12**, 4247

Insights into the mechanisms of biochar-derived dissolved organic carbon-facilitated transport of oxytetracycline in saturated porous media

Taotao Lu, [a] Xiaochen Liu,[b] Xiaochen Peng,[b] Yuqian Jin,[c] Sven Frei,[d] Jianqiang Lu*[e] and Shuangcheng Tang*[a]

Biochar-derived dissolved organic carbon (BDOC) may influence the environmental fate and behavior of tetracycline antibiotics in subsurface environments. In this study, BDOC derived from the pyrolysis of wheat straw at three distinct temperatures (300 °C, 450 °C, and 600 °C) was used to investigate its influence on the transport of oxytetracycline (OTC) through saturated quartz sand. The findings demonstrated that BDOC enhanced OTC mobility due to steric hindrance caused by organic matter accumulation, competition for retention sites between OTC and BDOC, and increased electrostatic repulsion between anionic species, including OTC^- ions and quartz sand. Notably, the mobility-enhancing effects of BDOC became significantly more pronounced at higher pyrolysis temperatures, likely resulting from increased organic matter deposition on sand surfaces and intensified electrostatic interactions. However, the promoting effect of BDOC on OTC transport was attenuated as pH increased from 5.0 to 9.0, which was attributed to reduced competitive deposition and steric effects caused by BDOC retention. Furthermore, cation-bridging, particularly with Cu^{2+} in the background solution, amplified BDOC's promotion effects. These results highlight that dissolved organic carbon released from biochar exerts a notable influence on the antibiotics' mobility within the aquifers.

Received 19th May 2025,
Accepted 12th August 2025

DOI: 10.1039/d5en00495k

rsc.li/es-nano

Environmental significance

This study highlights the critical role of biochar-derived dissolved organic carbon (BDOC) in influencing the environmental behavior of antibiotics, specifically oxytetracycline (OTC), in porous media. The findings demonstrate that BDOC enhances the mobility of OTC through mechanisms such as electrostatic repulsion, steric hindrance, and competitive interactions, which are affected by temperature, pH, and the presence of metal ions. These results underscore the importance of incorporating BDOC dynamics into environmental risk assessments to improve their predictive accuracy. The insights gained are essential for the design and optimization of biochar-based remediation strategies, ensuring their effectiveness and safety in real soil and water systems.

1. Introduction

Biochar, produced through the thermal decomposition of biomass under oxygen-limited (anoxic or hypoxic) conditions,[1,2] is a highly efficient and environmentally friendly carbon-based material, with wide applications in agriculture and environmental management, including soil remediation and pollutant removal from diverse water sources,[3,4] partly due to its excellent properties including large specific surface area, high cation exchange capacity, low cost, and the presence of numerous surface functional groups.[5,6] However, as biochar is increasingly applied to agricultural and contaminated soils for carbon sequestration and soil improvement, the leaching of BDOC into groundwater raises growing environmental concerns.[7–9] Numerous studies have demonstrated that BDOC possesses high stability and mobility in aquatic environments,[10,11] and can interact with various environmental contaminants, such as amine and phenolic compounds, antibiotics, and heavy metals.[12–14] Thus, these organic substances may affect the mobility, deposition, adsorption, and environmental fate of contaminants in soil–water systems.[15,16]

[a] *College of Hydraulic Science and Engineering, Yangzhou University, Yangzhou, 225009, P. R. China. E-mail: Tangsc@yzu.edu.cn*
[b] *Hydrogeology and Engineering Geology Institute of Hubei Geological Bureau, Jinzhou, 434020, P. R. China*
[c] *Survey and Design Institute Co., Ltd., Zhejiang Qiantang River Management Bureau, Hangzhou 310016, P. R. China*
[d] *Aquatic Ecology and Water Quality Management Group, Department of Environmental Science, Wageningen University Research Centre, Wageningen, 6700AA, The Netherlands*
[e] *Shangpu Gate Operation and Management Center in Shangyu District, Shaoxing, 312300, China. E-mail: jianqianlu.zj@gmail.com*

Given these effects, understanding how BDOC influences the transport of typical contaminants is essential for developing effective risk management and control strategies when using biochar in environmental and agricultural applications.

Oxytetracycline (OTC) is a broad-spectrum antimicrobial agent known for its potent bacteriostatic activity. It is extensively utilized as an effective medicine for treating human and animal diseases.[17] However, this drug undergoes incomplete metabolism in living organisms, and its metabolites are excreted and subsequently released into the environment,[18,19] where these compounds may have detrimental effects on human health, animal welfare, non-target organisms, and ecosystems.[20] Up to now, OTC has been increasingly detected in the natural environment.[21] Recently, this antibiotic has been reported to have the highest concentration (32.0 mg L^{-1}) in wastewater during antibiotic manufacturing.[22] Moreover, the concentrations of OTC in livestock manures have been determined to fall within the range of 17 to 18.54 mg kg^{-1}.[23] Notably, OTC discharged into soil, sediment, and surface water can potentially leach into groundwater systems,[24] resulting in irreversible changes in groundwater quality.[25,26] Given these concerns, a comprehensive investigation of the mobility characteristics of OTC within the water–soil environment is imperative and pivotal for elucidating the environmental fate and conducting an accurate risk assessment of this antibiotic.[21]

Numerous studies have been conducted in recent years to investigate the movement and retention characteristics of OTC within aquifer systems.[27–30] The findings obtained from these works displayed notable mobility within porous media characterized by quartz sand, sandy soil, and loamy soil.[29,30] Moreover, the enhancement of OTC transport through porous media has been attributed to colloidal substances like microplastics or engineered nanoparticles (*e.g.*, carbon nanotubes), which is ascribed to the carrier effect provided by these substances, along with the competitive deposition phenomena.[28,30] Additionally, our recent study revealed that the impact of rhamnolipid, a prototypical biosurfactant, on OTC behavior significantly varied with biosurfactant concentrations (1–10 mg L^{-1}) and was influenced by the chemical heterogeneities of aquifers.[31] Given that OTC molecules can form strong associations with dissolved organic carbon (DOC) through various processes, such as hydrogen bonding, hydrophobic interactions, and π–π interactions,[32–35] it is anticipated that DOC will affect the transport and deposition characteristics of this compound. In addition, compared with other dissolved organic matter (DOM), less attention has been paid to the BDOC, which differs from natural DOM in both composition and environmental behavior. BDOC is typically enriched in aromatic, redox-active, and thermally altered compounds, which can alter sorption behavior, enhance mobility, or even participate in redox transformations of pollutants.[36–38] Thus, BDOC may exert a more pronounced influence on contaminant transport. Nevertheless, the role of biochar-derived dissolved organic carbon (BDOC) in regulating OTC fate remains poorly understood. Further research is urgently needed to elucidate BDOC-mediated OTC transport mechanisms in groundwater systems.

This study systematically investigated the co-transport behavior of biochar-derived dissolved organic carbon (BDOC) and tetracycline antibiotics (*e.g.*, oxytetracycline, OTC) in saturated porous media. Transport experiments were conducted using various BDOC samples extracted from biochars produced by pyrolyzing wheat straw at temperatures ranging from 300 to 600 °C. In addition, several spectroscopic techniques were employed to characterize the physicochemical properties of these representative organic substances. Furthermore, a broad range of pH values (5.0–9.0) and the inclusion of Cu^{2+} ions were chosen to further investigate the impact of aqueous environmental factors on the BDOC-mediated transport of OTC. The underlying mechanisms governing BDOC-OTC co-transport are critical for predicting antibiotic mobility and designing risk management strategies in biochar-amended environments.

2. Materials and methods

2.1. Materials

Quartz sand with a grain diameter of 200–300 μm was obtained from Sigma-Aldrich (Bornem, Belgium). The average diameter of the sample was 260 μm. The purification methodology for the quartz sand followed our previous research.[39] Briefly, the grains underwent sequential washing steps with 0.1 M HCl, 5% H_2O_2, and deionized water (DI water). After washing, the quartz sand grains were dried at 90 °C in an oven. In order to clarify the surface charges of sand grains under different solution chemistry conditions, the ζ-potential values of the sand grains under different experimental conditions were measured using a Nano ZS 90 Zetasizer (Malvern Instruments Ltd., UK), following the method described by Mitropoulou *et al.*[40] Further operational details can be referenced in the SI, specifically in section S1.

Oxytetracycline (OTC) with a purity greater than 99% was obtained from Aladdin Biochemical Technology Co., Ltd. (Shanghai, China). The physicochemical characteristics of OTC are detailed in Table S1 and are available in the online supplementary material. To prepare the OTC solution, the powder form was dissolved into DI water, achieving a concentration of 100 g L^{-1}. Subsequently, the solution was preserved at 4 °C in a cold room. All other reagents, including NaCl, HCl, $CuCl_2$, and NaOH, were of analytical reagent (AR) grade.

2.2. Preparation of biochars

Wheat straw was collected from farmland in Henan province, northern China. Initially, the straw underwent rinsing with DI water to eliminate debris. Subsequently, the cleaned straw was dried in a hot air oven, maintaining a temperature of 80 °C. Following drying, the feedstock was subjected to pyrolysis at three distinct temperatures (*i.e.*, 300 °C, 450 °C, and 600 °C) using a conventional quartz tube furnace (O-KTF1200, Jiangsu, China). The process was maintained at each designated temperature for 3 hours, with a heating rate of 20 °C min^{-1}. The air-limited condition was achieved by omitting the use of carrier gas. Before employing the sample in

thermochemical conversion processes, the tube was initially filled with approximately 8 L of air at atmospheric pressure and ambient temperature. After cooling to ambient temperature, the sample was collected. It was then subjected to milling in a ball mill under dry conditions, followed by sieving through a 100-mesh sieve.

2.3. Extraction of BDOC

The BDOC was extracted following a previously described procedure.[41] Specifically, 10 g of biochar powder was added to containers filled with 200 mL DI water. These containers were securely sealed and subjected to continuous agitation at a constant speed of 100 rpm, maintained at a temperature of 20 °C for 3 days to facilitate interaction between the biochar and aqueous medium. Following the agitation phase, the mixtures were allowed to settle undisturbed for 3 h to enable the separation of suspended particles. The remaining aqueous suspensions were then filtered using 0.45 μm filters for the removal of undissolved or larger particulate matter. The concentrations of BDOC in the solutions were analyzed by a Shimadzu total organic carbon analyzer (TOC-VT). The BDOC derived from biochars produced at specific pyrolysis temperatures (300 °C, 450 °C, and 600 °C) were labeled as BDOC_300, BDOC_450, and BDOC_600, respectively.

2.4. BDOC characterization

A BDOC solution with a concentration of 10 mg L^{-1} was analyzed using a TU-1810PC UV spectrophotometer (Purkinje, China) to obtain its UV-vis absorbance characteristics. Absorbance measurements were recorded at a wavelength resolution of 1 nm. From the obtained spectral data, the key indicators, such as $SUVA_{254}$ (L mg_C^{-1} m^{-1}) and $S_{275–295}$, were derived (detailed information is provided in section S2 of the SI).[42] Additionally, a portion of the BDOC sample was freeze-dried and subsequently analyzed for its elemental composition and spectral properties. The specific weight percentages (wt%) of C, H, O, S, and N were determined using an elemental analyzer (Flash EA1112, Thermo Fisher Scientific). Surface chemical analysis was conducted *via* X-ray photoelectron spectroscopy (XPS) using an ESCALAB 250XI X-ray photoelectron spectrometer (Thermo Electron, USA). Fourier transform infrared (FTIR) spectra were recorded through an infrared spectrophotometer (Nicolet 6700, Thermo Fisher Scientific) over the wavenumber range of 400 to 4000 cm^{-1} with 2 cm^{-1} stepwise increments.

2.5. Transport experiments

The OTC transport in porous media was investigated through sand column experiments, focusing on understanding the influence of BDOC. ~15 g pretreated dry sand grains were meticulously packed into a robust borosilicate glass tube with an internal diameter of 1.1 cm and a length of 10.3 cm, ensuring uniform distribution throughout the column. The porosity of the packed sand columns was determined to be 0.42 ± 0.01. At the initiation of the experiment, the column was saturated by injecting 20 pore volumes (PV) of DI water at a constant flow rate of 0.27 cm min^{-1}, using a syringe pump (LSP01-1A, Baoding Longer Precision Pump Co., Ltd.) *via* an up-flow method.[43–45] Then, the sand column was flushed with 20 PV of electrolyte solution to standardize the chemical condition. Finally, ~17 PV of the influent, which contained either 5 mg L^{-1} OTC, 5 mg L^{-1} BDOC, or 1 mg L^{-1} OTC with 10 mg L^{-1} BDOC, along with a defined electrolyte composition, was introduced into the column using the syringe pump at the same flow rate.[44] These solutions were formulated by diluting stock solutions of BDOC and/or OTC in DI water enriched with designated electrolytes, and their pH was adjusted using 0.1 M NaOH or HCl. Note that the concentrations of electrolytes were used in this work according to the previous studies about the transport of environmental pollutants (*e.g.*, antibiotics and engineering nanoparticles) in porous media.[28,46–49] Meanwhile, effluent samples (~3.5 mL) were collected at ~30 minute intervals for BDOC and OTC concentration analysis. For single-component mobility experiments, the BDOC or OTC concentrations were quantified by the pre-established calibration lines (refer to Fig. S1).[50] For the co-mobility experiments, the concentrations of BDOC were also determined by measuring its absorbance using a UV-vis spectrometer at a wavelength of 430 nm (Fig. S1), a wavelength specifically selected due to OTC's negligible absorbance at this wavelength (Fig. S2).[51] Meanwhile, the concentrations of OTC were determined using a high-performance liquid chromatography system (e2695, Waters Alliance) following solvent extraction. Detailed procedures for the extraction and analysis are provided in the SI (section S3). All column experiments were performed in at least duplicate to ensure reproducibility and reliability of the results.

3. Results and discussion

3.1. Characteristics of BDOC

The essential physicochemical parameters of the obtained BDOC are presented in Fig. 1 and detailed in Table 1. As the pyrolysis temperature increased from 300 °C to 600 °C, the C content decreased from 21.96% to 13.20% (refer to Table 1). This decline is primarily attributed to the oxidation of carbon fractions within the biomass and the production of volatile compounds, including CO and CO_2, under conditions of limited oxygen availability.[52] Furthermore, the O content exhibited a decline from 35.85% to 18.59% with an increase in pyrolysis temperature. This reduction can be attributed to the heightened pyrolysis temperature, which promotes the volatilization of compounds through decarboxylation and demethylation. As a result, there was a decrease in surface oxygen-containing functional groups.[53] Note that both the H/C ratio, which serves as a measure of aliphaticity,[54] and the O/C ratio, indicative of polarity,[55] also displayed a downward trend as pyrolysis temperatures increased. This demonstrates that both aliphaticity and polarity of the BDOC decreased with rising temperature.[56,57] Furthermore, the $SUVA_{254}$ value obtained from ultraviolet spectral data reflects the aromaticity level of the organic substance, with a lower $SUVA_{254}$ value signifying a decrease in aromatic intensity.[57,58]

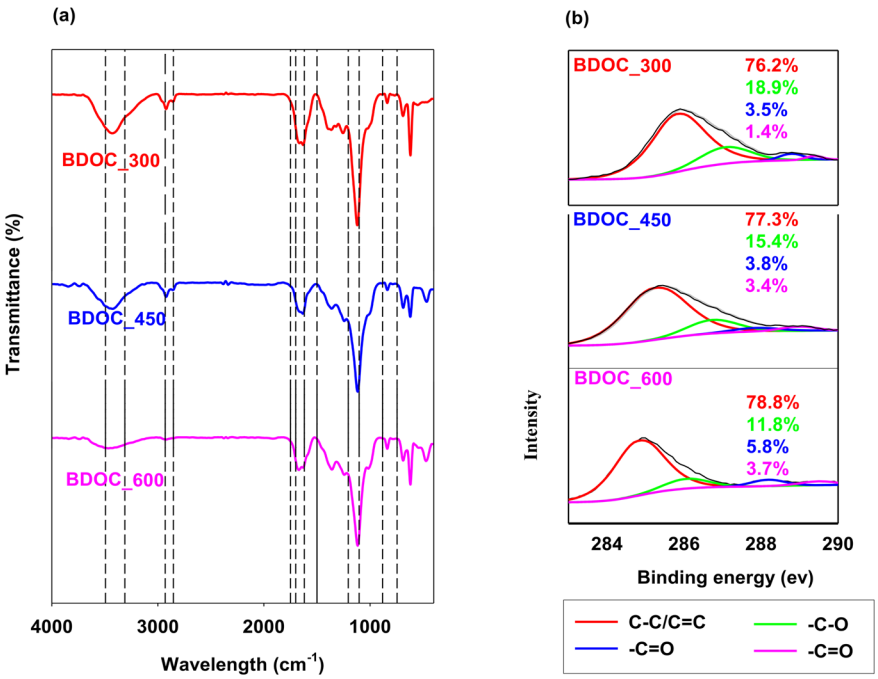

Fig. 1 (a) Fourier transform infrared spectra of biochars (the assignments of functional groups were shown in Table S2); (b) X-ray photoelectron spectroscopy (XPS) spectra of biochar. Four pseudo-subpeaks were identified and quantified in the C 1s spectra: 284.8 eV (C–C/C═C bonds), 286.5 eV (C–O bonds), and 288.1 eV (C═O bonds), and 289.7 eV (O–C═O bonds).

Table 1 Elemental compositions and amorphous carbon structure proportion of biochar-derived dissolved organic matter

	Bulk element composition							Surface element composition					
BDOC[a]	C (wt%)	O (wt%)	N (wt%)	H (wt%)	S (wt%)	O/C[b]	H/C[b]	C (at%)	O (at%)	N (at%)	O/C[c]	$SUVA_{254}$	$S_{275-295}$
BDOC_300	21.96	35.85	0.28	1.39	3.45	1.22	0.76	44.54	53.09	2.37	1.19	11.65	0.015
BDOC_450	17.48	26.68	0.2	1.01	2.84	1.14	0.69	39.98	59.25	1.17	1.48	13.47	0.017
BDOC_600	13.20	18.59	0.15	0.71	2.96	1.05	0.65	30.58	67.83	1.59	2.22	15.48	0.022

[a] "BDOC" presents wheat straw biochar-derived dissolved organic matter; the suffixes range from 300 to 600 represent the pyrolysis temperature. [b] Bulk atomic ratio, O/C: atomic ratio of oxygen to carbon, H/C: atomic ratio of hydrogen to carbon. [c] Surface atomic ratio of oxygen to carbon.

Additionally, the $SUVA_{254}$ values of BDOC increased with the rise in pyrolysis temperature (Table 1), which was consistent with the trend observed in the aliphaticity indicator, specifically the variations in H/C values. Meanwhile, studies have demonstrated that as the molecular size of DOC decreases, there is a corresponding rise in $S_{275-295}$ values.[59,60] In this study, the values of $S_{275-295}$ for BDOC exhibited an increase from 0.015 to 0.022 as pyrolysis temperatures rose from 300 °C to 600 °C (as shown in Table 1), indicating a reduction in the molecular size of BDOC at higher temperatures. Moreover, the FTIR analysis of BDOC revealed the presence of various surface functional groups in these organic compounds (Fig. 1a). For instance, the absorbance peak observed within the 1100–1250 cm^{-1} range was attributed to the vibration of the nitrogen-based functional groups (Table S2).[61] The absorption bands detected at 1700–1750 cm^{-1} and 3300–3490 cm^{-1} confirmed the presence of C═O and –OH groups, respectively.[59,62] The findings from the XPS revealed a reduction in the overall abundance of oxygen-containing functional groups on the surface, such as –C–O, –COO, and –C═O, as pyrolysis temperatures increased. Conversely, an inverse trend was noted in the content of C–C/C═C bonds (Fig. 1b), pointing to the thermal breakdown of surface functional groups as biomass pyrolysis progressed.[63]

3.2. BDOC-mediated transport of OTC in porous media

The influences of BDOC on OTC transport are illustrated in Fig. 2. Generally, BDOC demonstrated a capacity to facilitate OTC mobility. Notably, the maximum C/C_0 values (*i.e.*, the ratio of antibiotic concentration in the effluent, C, to the antibiotic concentration in the influent, C_0) of OTC increased from 81.9 ± 1.4% (without BDOC) to 89.1 ± 0.7% (with BDOC_600) (Table 2). This phenomenon can be primarily

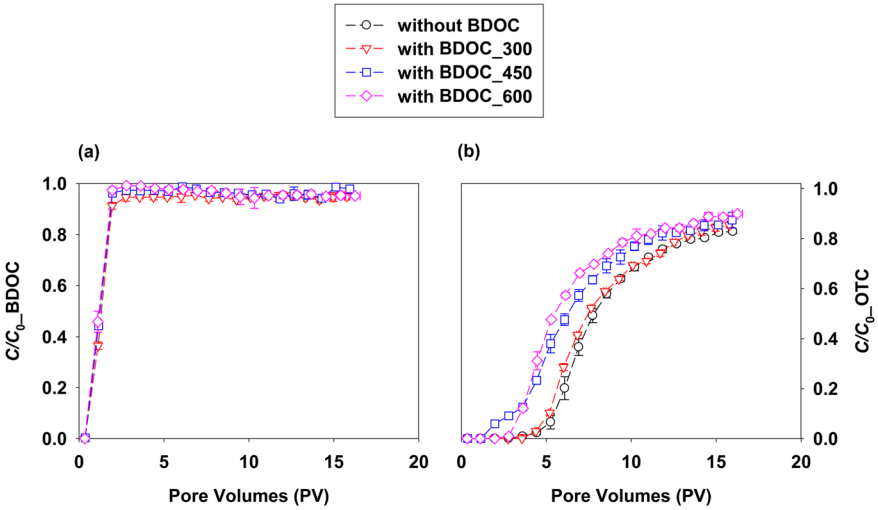

Fig. 2 Co-transport of BDOC and OTC (in 1 mM NaCl at pH 7.0) in saturated sand columns: (a) breakthrough curves of BDOC (columns 2–4, Table 2) and (b) breakthrough curves of OTC (columns 1–4, Table 2).

Table 2 Experimental setups and breakthrough results of column experiments

Column no.	Influent properties				Effluent properties[c]		The retained mass of BDOC in column[e] (%)	The retained mass of OTC in column[e] (%)
	BDOC[a]	OTC conc.[b] (mg L^{-1})	Background solution	pH	C/C_0[d]_ BDOC (%)	C/C_0_OTC (%)		
1	—	5	10 mM NaCl	7.0	—	81.9 ± 1.4	—	57.2 ± 1.1
2	BDOC_300	5	10 mM NaCl	7.0	94.4 ± 0.7	82.6 ± 1.2	13.4 ± 0.1	56.4 ± 0.1
3	BDOC_450	5	10 mM NaCl	7.0	96.9 ± 2.3	86.1 ± 1.2	11.0 ± 0.3	47.0 ± 1.6
4	BDOC_600	5	10 mM NaCl	7.0	95.2 ± 0.2	89.1 ± 0.7	10.7 ± 0.7	43.6 ± 0.6
5	BDOC_450	—	10 mM NaCl	7.0	94.8 ± 0.9	—	14.6 ± 0.1	—
6	BDOC_450	—	10 mM NaCl	5.0	89.1 ± 0.2	—	26.0 ± 0.6	—
7	—	5	10 mM NaCl	5.0	—	47.4 ± 2.5	—	81.5 ± 0.1
8	BDOC_450	5	10 mM NaCl	5.0	90.1 ± 0.4	60.3 ± 3.7	24.4 ± 0.4	63.2 ± 0.1
9	BDOC_450	—	10 mM NaCl	9.0	96.9 ± 0.2	—	13.9 ± 0.3	—
10	—	5	10 mM NaCl	9.0	—	91.7 ± 0.4	—	29.3 ± 0.2
11	BDOC_450	5	10 mM NaCl	9.0	93.6 ± 0.9	11.4 ± 1.3	98.4 ± 0.5	26.4 ± 0.1
12	BDOC_450	—	0.1 mM $CuCl_2$	5.0	68.7 ± 0.4	—	42.1 ± 0.3	—
13	—	5	0.1 mM $CuCl_2$	5.0	—	14.3 ± 1.4	—	95.8 ± 0.3
14	BDOC_450	5	0.1 mM $CuCl_2$	5.0	70.7 ± 0.5	20.6 ± 0.8	36.3 ± 0.6	90.8 ± 1.1

[a] "BDOC" presents wheat straw biochar-derived dissolved organic carbon; the suffixes range from 300 to 600 represent the pyrolysis temperature. [b] Conc. represent concentration. [c] Average value of last three data points of respective breakthrough curve. [d] C/C_0 denotes the normalized effluent concentration. [e] Mass retained in column = 100 − effluent mass.

attributed to several factors. Firstly, BDOC can be deposited on sand surfaces through multiple mechanisms, such as H-bonding (*via* the ≡Si–OH groups of sand surfaces and the deprotonated –COOH of BDOC), hydrophobic, and electrostatic forces.[64,65] In this scenario, BDOC and OTC molecules engaged in competition for the adsorption sites on the surface of sand grains. As a result, the accumulation of BDOC reduced the number of available sites for effective OTC adsorption,[33,46,66] ultimately leading to improved mobility of OTC. Secondly, BDOC has the capacity to form associations with OTC molecules *via* π–π interactions, H-bonding, and hydrophobic contacts.[32–35] Consequently, the steric hindrance, a molecular-scale repulsion, between OTC molecules and quartz sand particles could be amplified by BDOC adsorption onto sand grains and interactions with OTC, due to BDOC macromolecules occupying interfacial spaces, altering local pore structures, or forming spatial barriers.[32,67–70] Thirdly, as shown in Fig. S3, a fraction of OTC molecules existed in their deprotonated (anionic) form (OTC^-, 25.7%) in the aqueous phase at pH 7.0. At the same time, the quartz sand exhibited negatively charged at pH 7.0 (Table S3). Hence, an electrostatic repulsion existed between OTC molecules and sand grains, which contributed to OTC movement.[66,71,72] Table S3 revealed a shift towards a more negative surface charge on sand grains with BDOC presence. Therefore, the addition of BDOC exhibited a facilitating influence on OTC mobility, attributed to the enhanced electrostatic repulsion.[46,66,67,73]

Furthermore, as mentioned above, BDOC produced at lower temperatures had a small molecular size. Intuitively, smaller-sized BDOC exhibited a higher mobility due to the decrease of the straining effect.[59,74,75] However, in this work, irrespective of the presence or absence of OTC, the mobility of BDOC exhibited a slight increase with ascending pyrolysis temperature (Fig. 2a and S4 and Table 2). As noted above, the polarity of BDOC decreased while its aromaticity increased with rising pyrolysis temperature. At the same time, the abundance of organic functional groups on the BDOC surface declined, as shown in Fig. 1. More importantly, certain functional groups (*e.g.*, –COOH groups) could deprotonate at pH 7.0 in this work.[59,76,77] Hence, the pronounced mobility of BDOC produced at lower temperatures could be attributed to the weaker hydrophobic interaction as well as the stronger electrostatic repulsion between the dissociated BDOC molecules and the negatively charged quartz sand grains (Table S3).[61,78–80] Interestingly, the mobility-enhancing effects of BDOC considerably depended on the BDOC species. That is, the observed enhancement generally aligned with the order BDOC_600 > BDOC_450 > BDOC_300 (Fig. 2b). The observed pattern may be explained by several underlying mechanisms. On the one hand, as discussed earlier, the aromaticity of BDOC increased with rising pyrolysis temperature. As a result, compared to the other two organic matters, more BDOC_600 could contact OTC molecules due to the stronger hydrophobic interactions (*e.g.*, hydrophobic and π–π stacking interactions).[32,34,35] Consequently, the most pronounced steric hindrance effect was observed in the case of BDOC_600, leading to the most significantly enhanced

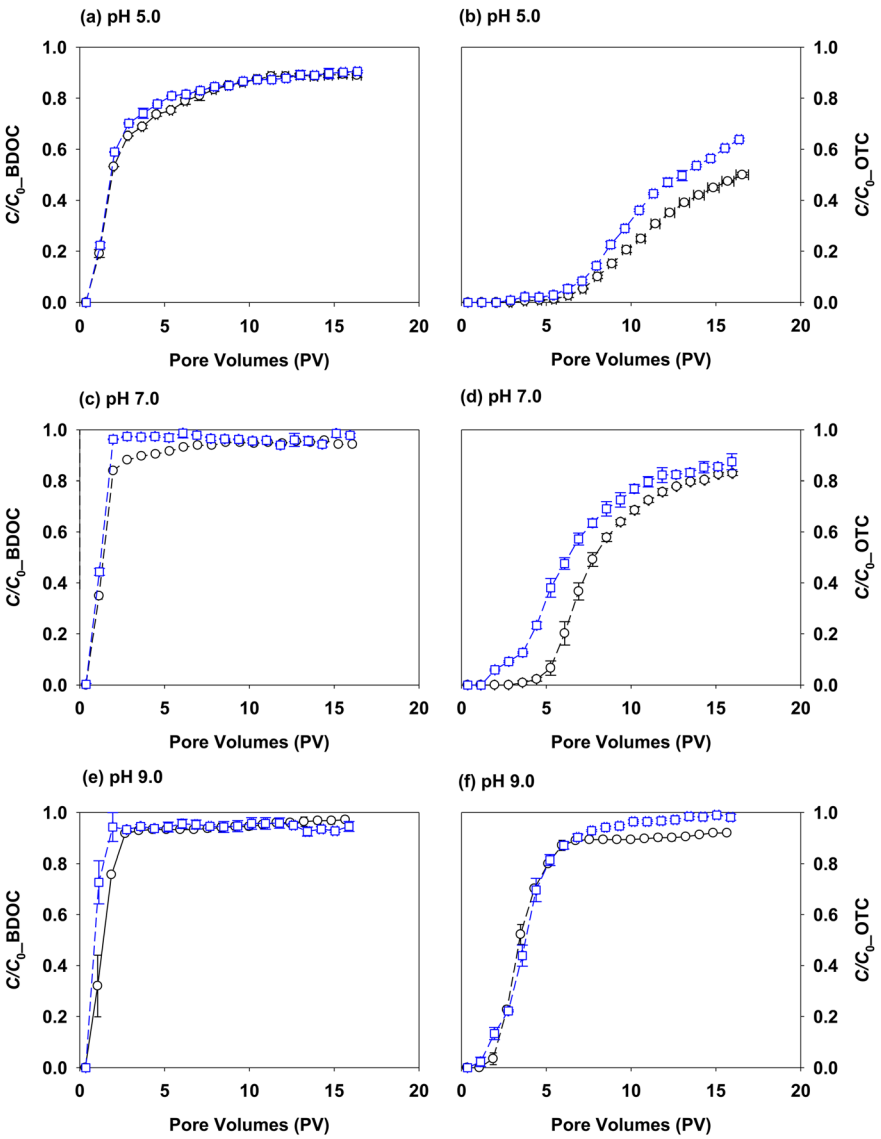

Fig. 3 Co-transport of BDOC_450 and OTC in saturated soil columns at different pH conditions (the ionic strength was 10 mM NaCl): (a) and (b) breakthrough curves of BDOC and OTC at pH 5.0 (columns 6–8, Table 2), respectively; (c) and (d) breakthrough curves of BDOC and OTC at pH 7.0 (columns 1, 3, and 5, Table 2), respectively; and (e) and (f) breakthrough curves of BDOC and OTC at pH 9.0 (columns 9–11, Table 2), respectively.

effect of this BDOC on OTC mobility.[66] On the other hand, the quartz sand displayed the highest negative ζ-potential in the case of BDOC_600 among the three BDOC variants (Table S3). Hence, the pronounced electrostatic repulsion force between the anionic forms of OTC and sand grains significantly contributed to the enhanced mobility of OTC observed with BDOC_600.[46,81]

3.3. Impact of pH on BDOC-mediated transport of OTC

The co-transport of BDOC (choosing BDOC_450 as the model BDOC) and OTC at three different pH values (5.0, 7.0, and 9.0) were also explored (Fig. 3). In general, BDOC exhibited the potential to enhance the transport of OTC across diverse pH conditions. The mechanistic basis for BDOC-mediated enhancement of OTC mobility is attributed to a combination of (1) amplified electrostatic repulsion between negatively charged OTC species and sand particles, (2) steric hindrance impeding adsorption interactions, and (3) competitive retention dynamics favoring BDOC over OTC at binding sites.[32,33,46,66,71]

Intriguingly, the enhancement of OTC transport by BDOC_450 demonstrated pH-dependent attenuation, progressively diminishing under elevated pH conditions (from 5.0 to 9.0). As shown in Table 2 and Fig. 3, the retained mass of OTC decreased by 22.5% (from 81.5 ± 0.1% (in the absence of BDOC_450) to 63.2 ± 0.1% (in the presence of BDOC_450)), 17.8% (from 57.2 ± 1.1% to 47.0 ± 0.6%), and 9.9% (from 29.3 ± 0.2% to 26.4 ± 0.1%) when background solution pH values were 5.0, 7.0, and 9.0, respectively. This phenomenon was related to the varied deposition capacities of BDOC onto sand grains at different solution pH values. As demonstrated in Table S3, the surface charge of sand particles exhibited increasing negative character under elevated pH conditions, evidenced by ζ-potential progressively decreasing from −32.7 ± 1.3 mV (pH 5.0) to −55.1 ± 0.8 mV (pH 9.0). The surfaces of BDOC molecules exhibited enhanced negative surface charge under elevated pH conditions, attributed to the deprotonation of ionizable functional groups, including–COOH and–OH moieties, thereby strengthening electrostatic repulsion forces.[54,82] In this instance, the retention of BDOC in the sand column diminished with the rise in solution pH, primarily because of enhanced electrostatic interaction. This, in turn, diminished both steric hindrance and the competitive retention that existed between BDOC and OTC. Thus, the facilitative impact of BDOC was more pronounced under acidic conditions compared to alkaline environments.

Furthermore, the mobility of BDOC was enhanced as the pH values of the solution were raised (Fig. S5). This observation primarily originated from the surface charges of both sand particles and BDOC molecules. It is worth noting that the ζ-potential values of sand grains demonstrated an increased negativity at high pH values (Table S3). Also, BDOC molecule surfaces possessed greater negative charges at elevated pH levels, a result of deprotonating organic functional groups.[54,80,82] Consequently, the increased electrostatic repulsion between BDOC and sand grains could facilitate BDOC transport at a high pH.[7,59,83] Moreover, the transport of OTC demonstrated an increase with increasing solution pH values, observed under both BDOC-addition and BDOC-free conditions (Fig. S6). The results are mainly ascribed to the species transformations of OTC molecules prompted by variations in solution pH.[29,84] As demonstrated in Fig. S3, with the elevation of pH from 5.0 to 9.0, the presence of OTC molecules in their anionic forms, OTC^- and OTC^{2-}, notably increased. Thus, the intensified electrostatic repulsion between anionic OTC species and sand particles further enhanced the mobility of this antibiotic at higher pH levels.[84–86] Moreover, it is worth noting that the observed decline in BDOC's facilitative effect at higher pH does not solely result from reduced BDOC retention. As pH increases, OTC itself becomes more mobile due to its transformation into anionic forms, which experience stronger electrostatic repulsion from the sand surface. Consequently, the baseline mobility of OTC increases with pH, reducing the relative contribution of BDOC to further enhancing its transport. In this situation, although BDOC remains more mobile at higher pH and may still contribute to OTC transport, its net facilitative effect becomes less pronounced because OTC migration is already substantially elevated under alkaline conditions.

3.4. BDOC-mediated transport of OTC in the presence of divalent cations

Besides monovalent cations (*e.g.*, Na^+ and K^+), certain divalent cations, such as Ca^{2+}, Mg^{2+}, Pb^{2+}, and Cu^{2+}, are abundant in subsurface environments,[87] which may affect the transport and fate of tetracycline antibiotics.[88,89] Thus, research into the mobility of OTC in the shadow of divalent cations would be beneficial in learning more about the deposition mechanism of this antibiotic in aquifer media. Mobility of OTC in the presence of Cu^{2+} (a representative divalent cation) mediated by BDOC_450 is depicted in Fig. 4. Similar to observations with Na^+, BDOC also enhanced OTC mobility in the background solution containing Cu^{2+}. As detailed in Table 2, the retained mass of OTC in the column decreased from 95.8 ± 0.3% (without BDOC_450) to 90.8 ± 1.1% (with BDOC_450). The main mechanisms controlling the co-mobility of BDOC and OTC in quartz sand columns were closely consistent with those described in section 3.2.

Notably, the OTC transport was significantly enhanced in the presence of 0.3 mM Na^+ compared to 0.1 mM Cu^{2+}, despite the similar ionic strengths of the two solutions, as shown in Fig. S7. As mentioned previously, functional groups were present on the surfaces of both the sand grain and OTC molecules. Consequently, the cation-bridging effect exerted by Cu^{2+} demonstrated a marked influence on the co-mobility of OTC and BDOC when compared to Na^+.[61,67,90,91] Specifically, the adsorption of Cu^{2+} onto quartz sand surfaces created supplementary reactive sites for OTC deposition

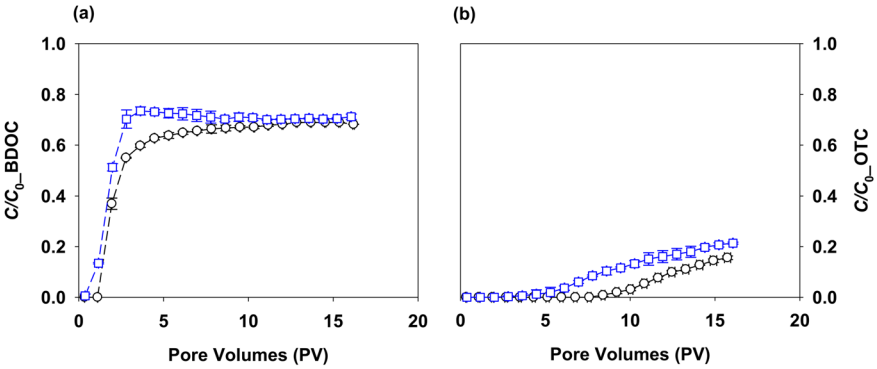

Fig. 4 Co-transport of BDOC_450 and OTC in saturated soil columns in the presence of 0.1 mM Cu^{2+} (pH 5.0): (a) and (b) breakthrough curves of BDOC_450 and OTC (columns 12 and 13, Table 2), respectively.

through metal ion coordination, facilitating the formation of ternary surface complexes (sand–Cu^{2+}–OTC).[29,88,89,92,93] Meanwhile, Cu^{2+} ions functioned as cationic bridging mediators, facilitating interfacial binding between ionized functional groups (–COOH) on BDOC molecules and sand surfaces through the formation of supramolecular assemblies,[94–96] which led to more BDOC molecules being deposited on the sand surfaces. These findings established the cation-bridging effect as the main mechanism controlling the OTC transport under the influence of BDOC in the presence of Cu^{2+}.

4. Conclusions

Recently, biochar has received significant attention owing to its potential environmental applications in various fields. Notably, this emerging carbon-based material exhibits a propensity for releasing BDOC under environmental conditions. More importantly, BDOC holds the potential to eventually influence the environmental behaviors of contaminants within both soil and aquatic systems. Therefore, understanding how these organic substances influence antibiotic mobility is critical for assessing and predicting the environmental fate and risks of organic pollutants. The findings obtained from this study demonstrate that BDOC could promote OTC transport in quartz sand arising from the heightened electrostatic repulsion between the anionic OTC species (*i.e.*, OTC^{-}/OTC^{2-}), and sand grains, the steric hindrance resulting from the BDOC retention and the competitive deposition interactions between OTC and BDOC. Meanwhile, the enhanced effects of BDOC obtained at higher temperatures (*e.g.*, 600 °C) exhibited greater mobility-enhancement effects, attributed to increased electrostatic repulsion and steric interactions. Notably, the transport-enhancing effects of BDOC diminished progressively with increasing pH ranging from 5.0 to 9.0. This pattern primarily resulted from the reduced competition for effective deposition sites and the weakened steric effect, both of which decreased BDOC deposition onto sand surfaces. Furthermore, the cation-bridging of OTC mobility when the solution contained Cu^{2+}. In summary, this study elucidates that BDOC substantially alters the transport and retention of tetracycline in porous media, underscoring the necessity of integrating BDOC interactions into the assessment and design of biochar-based environmental remediation strategies. It is important to note that the release characteristics of BDOC vary significantly with biochar type, which is influenced not only by feedstock source and pyrolysis temperature but also by factors such as heating rate, residence time, and pyrolysis atmosphere. These differences suggest that the BDOC behavior observed in this study may not be generalizable to all biochar types. Further systematic studies are needed to evaluate how these parameters affect BDOC dynamics. Additionally, natural environments contain various kinds of heavy metal ions (*e.g.*, Zn^{2+}, Ca^{2+}, Mn^{2+}, and Cr^{6+}). These metal ions may have significantly different influences on the mobility of tetracycline antibiotics. Thus, more studies are needed to understand the mobility of tetracycline antibiotics as a function of different metal ions. Meanwhile, in order to comprehensively understand the fate of antibiotics in groundwater systems, more environmental factors (*e.g.*, the moisture content of the aquifer, the porous media containing different minerals, the grain size, and flow rate) controlling DOM-mediated transport of OTC should be considered.

Conflicts of interest

The authors declare that there are no conflicts of interest in the present study.

Data availability

Supplementary information is available: The data supporting the findings of this study are available within the article and/or its SI. See DOI: **https://doi.org/10.1039/D5EN00495K**.

The authors declare that the data supporting the findings of this study are available within the paper and its SI. Should any raw data files be needed in another format they are available from the corresponding author upon reasonable request.

Acknowledgements

This project was supported by National Natural Science Foundation of China (Grant No. 32401403), and the Open Project of Key Laboratory of Groundwater Circulation and Environmental Evolution (China University of Geosciences (Beijing)), Ministry of Education.

References

1 J. Poerschmann, B. Weiner, H. Wedwitschka, A. Zehnsdorf, R. Koehler and F. D. Kopinke, Characterization of biochars and dissolved organic matter phases obtained upon hydrothermal carbonization of Elodea nuttallii, *Bioresour. Technol.*, 2015, **189**, 145–153.

2 Y. Xiong and E. Bi, Effect of endogenetic dissolved organic matter on tetracycline adsorption by biochar, *Environ. Sci. Pollut. Res.*, 2023, **30**, 77022–77031.

3 F. D. Meng, Q. X. Huang, Y. B. Cai, F. Y. Li and G. D. Yuan, Effects of biowaste-derived biochar on the dynamic behavior of cadmium fractions in soils, *Environ. Sci. Pollut. Res.*, 2022, **29**, 59043–59051.

4 A. Tomczyk, Z. Sokolowska and P. Boguta, Biochar physicochemical properties: pyrolysis temperature and feedstock kind effects, *Rev. Environ. Sci. Bio/Technol.*, 2020, **19**, 191–215.

5 N. Hao, J. Cao, J. Ye, C. Zhang, C. Li and B. Bate, Content and morphology of lead remediated by activated carbon and biochar: A spectral induced polarization study, *J. Hazard. Mater.*, 2021, **411**, 124605.

6 C. Wang, D. Luo, X. Zhang, R. Huang, Y. Cao, G. Liu, Y. Zhang and H. Wang, Biochar-based slow-release of fertilizers for sustainable agriculture: A mini review, *Environ. Sci. Ecotechnology*, 2022, **10**, 100167.

7 Y. Guo, Y. Guo, S. G. Hua, G. W. Xu, Z. X. Xu and C. C. Yan, Coupling band structure and oxidation-reduction potential to expound photodegradation performance difference of biochar-derived dissolved black carbon for organic pollutants under light irradiation, *Sci. Total Environ.*, 2022, **820**, 153300.

8 X. Qu, H. Fu, J. Mao, Y. Ran, D. Zhang and D. Zhu, Chemical and structural properties of dissolved black carbon released from biochars, *Carbon*, 2016, **96**, 759–767.

9 A. U. Rajapaksha, Y. S. Ok, A. El-Naggar, H. Kim, F. Song, S. Kang and Y. F. Tsang, Dissolved organic matter characterization of biochars produced from different feedstock materials, *J. Environ. Manage.*, 2019, **233**, 393–399.

10 S. J. Jiang, G. L. Dai, Z. Y. Liu, T. He, J. Zhong, Y. C. Ma and Y. H. Shu, Field-scale fluorescence fingerprints of biochar-derived dissolved organic matter (DOM) provide an effective way to trace biochar migration and the downward co-migration of Pb, Cu and As in soil, *Chemosphere*, 2022, **301**, 134738.

11 F. Yang, C. P. Wang and H. W. Sun, A comprehensive review of biochar-derived dissolved matters in biochar application: Production, characteristics, and potential environmental effects and mechanisms, *J. Environ. Chem. Eng.*, 2021, **9**, 105258.

12 F. Yang, Q. Zhu, Y. Gao, H. Jian, C. Wang and H. Sun, Effects of biochar-dissolved organic matter on the photodegradation of sulfamethoxazole and chloramphenicol in biochar solutions as revealed by oxygen reduction performances and free radicals, *Sci. Total Environ.*, 2021, **781**, 146807.

13 X. Guo, Y. Peng, N. Li, Y. Tian, L. Dai, Y. Wu and Y. Huang, Effect of biochar-derived DOM on the interaction between Cu(II) and biochar prepared at different pyrolysis temperatures, *J. Hazard. Mater.*, 2022, **421**, 126739.

14 Y. Guo, Y. Guo, S. Hua, G. Xu, Z. Xu and C. Yan, Coupling band structure and oxidation-reduction potential to expound photodegradation performance difference of biochar-derived dissolved black carbon for organic pollutants under light irradiation, *Sci. Total Environ.*, 2022, **820**, 153300.

15 D. Wan, J. Wang, D. D. Dionysiou, Y. Kong, W. Yao, S. Selvinsimpson and Y. Chen, Photogeneration of Reactive Species from Biochar-Derived Dissolved Black Carbon for the Degradation of Amine and Phenolic Pollutants, *Environ. Sci. Technol.*, 2021, **55**, 8866–8876.

16 S. Jiang, G. Dai, Z. Liu, T. He, J. Zhong, Y. Ma and Y. Shu, Field-scale fluorescence fingerprints of biochar-derived dissolved organic matter (DOM) provide an effective way to trace biochar migration and the downward co-migration of Pb, Cu and As in soil, *Chemosphere*, 2022, **301**, 134738.

17 J. Leichtweis, Y. Vieira, N. Welter, S. Silvestri, G. L. Dotto and E. Carissimi, A review of the occurrence, disposal, determination, toxicity and remediation technologies of the tetracycline antibiotic, *Process Saf. Environ. Prot.*, 2022, **160**, 25–40.

18 F. Huang, Z. An, M. J. Moran and F. Liu, Recognition of typical antibiotic residues in environmental media related to groundwater in China (2009-2019), *J. Hazard. Mater.*, 2020, **399**, 122813.

19 R. Lulijwa, E. J. Rupia and A. C. Alfaro, Antibiotic use in aquaculture, policies and regulation, health and environmental risks: a review of the top 15 major producers, *Rev. Aquac.*, 2020, **12**, 640–663.

20 R. A. Sversut, A. A. da Silva, T. F. M. Cardoso, N. M. Kassab, M. S. do Amaral and H. R. N. Salgado, A Critical Review of Properties and Analytical Methods for the Determination of Oxytetracyline in Biological and Pharmaceutical Matrices, *Crit. Rev. Anal. Chem.*, 2016, **47**, 154–171.

21 P. Kovalakova, L. Cizmas, T. J. McDonald, B. Marsalek, M. Feng and V. K. Sharma, Occurrence and toxicity of antibiotics in the aquatic environment: A review, *Chemosphere*, 2020, **251**, 126351.

22 A. S. Oberoi, Y. Jia, H. Zhang, S. K. Khanal and H. Lu, Insights into the Fate and Removal of Antibiotics in Engineered Biological Treatment Systems: A Critical Review, *Environ. Sci. Technol.*, 2019, **53**, 7234–7264.

23 Y.-J. Zhang, H.-W. Hu, M. Gou, J.-T. Wang, D. Chen and J.-Z. He, Temporal succession of soil antibiotic resistance genes following application of swine, cattle and poultry manures spiked with or without antibiotics, *Environ. Pollut.*, 2017, **231**, 1621–1632.

24 Y. J. Zhang, H. W. Hu, M. Gou, J. T. Wang, D. L. Chen and J. Z. He, Temporal succession of soil antibiotic resistance

genes following application of swine, cattle and poultry manures spiked with or without antibiotics, *Environ. Pollut.*, 2017, **231**, 1621–1632.

25 A. K. Sarmah, M. T. Meyer and A. B. A. Boxall, A global perspective on the use, sales, exposure pathways, occurrence, fate and effects of veterinary antibiotics (VAs) in the environment, *Chemosphere*, 2006, **65**, 725–759.

26 L. L. Yao, Y. X. Wang, L. Tong, Y. M. Deng, Y. G. Li, Y. Q. Gan, W. Guo, C. J. Dong, Y. H. Duan and K. Zhao, Occurrence and risk assessment of antibiotics in surface water and groundwater from different depths of aquifers: A case study at Jianghan Plain, central China, *Ecotoxicol. Environ. Saf.*, 2017, **135**, 236–242.

27 J. Fang, B. Shen, L. L. Cheng, M. H. Wang, L. Q. Zhang and D. H. Lin, Oxytetracycline increases the mobility of carbon nanotubes in porous media, *Sci. Total Environ.*, 2018, **628–629**, 1130–1138.

28 J. Fang, M. H. Wang, B. Shen, L. Q. Zhang and D. H. Lin, Distinguishable co-transport mechanisms of phenanthrene and oxytetracycline with oxidized-multiwalled carbon nanotubes through saturated soil and sediment columns: vehicle and competition effects, *Water Res.*, 2017, **108**, 271–279.

29 Y. H. Jin, M. Y. Liu, Q. Zhang, U. Farooq, W. F. Chen, T. T. Lu and Z. C. Qi, Transport of oxytetracycline through saturated porous media: role of surface chemical heterogeneity, *Environ. Sci.:Processes Impacts*, 2022, **24**, 2368–2377.

30 J. Li, K. Guo, Y. S. Cao, S. S. Wang, Y. Song and H. B. Zhang, Enhance in mobility of oxytetracycline in a sandy loamy soil caused by the presence of microplastics, *Environ. Pollut.*, 2021, **269**, 116151.

31 Y. Jin, J. Chen, Q. Zhang, U. Farooq, T. Lu, B. Wang, Z. Qi and W. Chen, Biosurfactant-affected mobility of oxytetracycline and its variations with surface chemical heterogeneity in saturated porous media, *Water Res.*, 2023, **244**, 120509.

32 P. Kulshrestha, R. F. Giese and D. S. Aga, Investigating the molecular interactions of oxytetracycline in clay and organic matter: Insights on factors affecting its mobility in soil, *Environ. Sci. Technol.*, 2004, **38**, 4097–4105.

33 L. L. Qiu, J. J. Wu, Y. Qian, M. Nafees, J. X. Zhang, W. C. Du, Y. Yin and H. Y. Guo, Impact of biochar-induced vertical mobilization of dissolved organic matter, sulfamethazine and antibiotic resistance genes variation in a soil-plant system, *J. Hazard. Mater.*, 2021, **417**, 126022.

34 C. Wang, H. Xu, T. Cheng, S. Tang, D. Zhang, M. Li and X. Pan, Affinity-based alleviation of dissolved organic matter (DOM) on tetracycline toxicity to photosynthesis of green algae Chlorella vulgaris: roles of hydrophilic and hydrophobic DOM, *Environ. Sci. Pollut. Res.*, 2023, **30**, 42165–42175.

35 B. L. Xu, F. Liu, P. C. Brookes and J. M. Xu, Microplastics play a minor role in tetracycline sorption in the presence of dissolved organic matter, *Environ. Pollut.*, 2018, **240**, 87–94.

36 B. Saletnik, G. Zagula, M. Bajcar, M. Tarapatskyy, G. Bobula and C. Puchalski, Biochar as a Multifunctional Component of the Environment A Review, *Appl. Sci.*, 2019, **9**, 1139.

37 Y. Q. Sun, X. N. Xiong, M. J. He, Z. B. Xu, D. Y. Hou, W. H. Zhang, Y. S. Ok, J. Rinklebe, L. L. Wang and D. C. W. Tsang, Roles of biochar-derived dissolved organic matter in soil amendment and environmental remediation: A critical review, *Chem. Eng. J.*, 2021, **424**, 130387.

38 B. P. Zhang, S. F. Zhou, L. H. Zhou, J. L. Wen and Y. Yuan, Pyrolysis temperature-dependent electron transfer capacities of dissolved organic matters derived from wheat straw biochar, *Sci. Total Environ.*, 2019, **696**, 133895.

39 M. Wang, Y. Song, H. Zhang, T. Lu, W. Chen, W. Li, W. Qi and Z. Qi, Insights into the mutual promotion effect of graphene oxide nanoparticles and tetracycline on their transport in saturated porous media, *Environ. Pollut.*, 2021, **268**, 115730.

40 P. N. Mitropoulou, V. I. Syngouna and C. V. Chrysikopoulos, Transport of colloids in unsaturated packed columns: Role of ionic strength and sand grain size, *Chem. Eng. J.*, 2013, **232**, 237–248.

41 J. Tang, X. Li, Y. Luo, G. Li and S. Khan, Spectroscopic characterization of dissolved organic matter derived from different biochars and their polycylic aromatic hydrocarbons (PAHs) binding affinity, *Chemosphere*, 2016, **152**, 399–406.

42 J. R. Helms, A. Stubbins, J. D. Ritchie, E. C. Minor, D. J. Kieber and K. Mopper, Absorption spectral slopes and slope ratios as indicators of molecular weight, source, and photobleaching of chromophoric dissolved organic matter, *Limnol. Oceanogr.*, 2008, **53**, 955–969.

43 C. H. Ko and M. Elimelech, The "shadow effect" in colloid transport and deposition dynamics in granular porous media: Measurements and mechanisms, *Environ. Sci. Technol.*, 2000, **34**, 3681–3689.

44 Y. Y. Sun, B. Gao, S. A. Bradford, L. Wu, H. Chen, X. Q. Shi and J. C. Wu, Transport, retention, and size perturbation of graphene oxide in saturated porous media: Effects of input concentration and grain size, *Water Res.*, 2015, **68**, 24–33.

45 M. Wang, C. R. Yu, D. S. Tang, J. J. Chen and B. Gao, Effects of Surfactant and Electrolyte Concentrations, Cation Valence, and Temperature on Graphene Oxide Retention and Transport in Saturated Porous Media, *Water, Air, Soil Pollut.*, 2019, **230**, 21.

46 D. Cheng, P. Liao and S. H. Yuan, Effects of ionic strength and cationic type on humic acid facilitated transport of tetracycline in porous media, *Chem. Eng. J.*, 2016, **284**, 389–394.

47 Y. N. Xing, X. J. Chen, X. Chen and J. Zhuang, Colloid-Mediated Transport of Pharmaceutical and Personal Care Products through Porous Media, *Sci. Rep.*, 2016, **6**, 35407.

48 L. L. Xu, Y. Liang, C. J. Liao, T. Xie, H. B. Zhang, X. Y. Liu, Z. W. Lu and D. J. Wang, Cotransport of micro- and nanoplastics with chlortetracycline hydrochloride in saturated porous media: Effects of physicochemical heterogeneities and ionic strength, *Water Res.*, 2022, **209**, 117886.

49 L. L. Zhang, D. Q. Zhu, H. Wang, L. Hou and W. Chen, Humic acid-mediated transport of tetracycline and pyrene in saturated porous media, *Environ. Toxicol. Chem.*, 2012, **31**, 534–541.

50 P. K. Ma, Z. C. Qi, X. Wu, R. Ji and W. Chen, Biochar nanoparticles-mediated transport of organic contaminants in porous media: dependency on contaminant properties and effects of biochar aging, *Carbon Res.*, 2023, **2**, 1–15.
51 G. Chen, X. Liu and C. Su, Distinct Effects of Humic Acid on Transport and Retention of TiO2 Rutile Nanoparticles in Saturated Sand Columns, *Environ. Sci. Technol.*, 2012, **46**, 7142–7150.
52 H. Zhang, W. Qian, L. Wu, S. Yu, R. Wei, W. Chen and J. Ni, Spectral characteristics of dissolved organic carbon (DOC) derived from biomass pyrolysis: Biochar-derived DOC versus smoke-derived DOC, and their differences from natural DOC, *Chemosphere*, 2022, **302**, 134869.
53 H. Luo, E. Almatrafi, W. Wang, Y. Yang, D. Huang, W. Xiong, M. Cheng, C. Zhou, Y. Zhou, Q. Lin, G. Fang, G. Zeng and C. Zhang, Insight into the effect of pyrolysis temperature on photoreactivity of biochar-derived dissolved organic matter: Impacts of aromaticity and carbonyl groups, *Sci. Total Environ.*, 2023, **871**, 162048.
54 H. Y. Zhang, W. Qian, L. Wu, S. H. Yu, R. Wei, W. F. Chen and J. Z. Ni, Spectral characteristics of dissolved organic carbon (DOC) derived from biomass pyrolysis: Biochar-derived DOC versus smoke-derived DOC, and their differences from natural DOC, *Chemosphere*, 2022, **302**, 134869.
55 J. Poerschmann, B. Weiner, H. Wedwitschka, A. Zehnsdorf, R. Koehler and F. D. Kopinke, Characterization of biochars and dissolved organic matter phases obtained upon hydrothermal carbonization of Elodea nuttallii, *Bioresour. Technol.*, 2015, **189**, 145–153.
56 H. Z. Luo, E. Almatra, W. J. Wang, Y. Yang, D. L. Huang, W. P. Xiong, M. Cheng, C. Y. Zhou, Y. Zhou, Q. Lin, G. G. Fang, G. M. Zeng and C. Zhang, Insight into the effect of pyrolysis temperature on photoreactivity of biochar- derived dissolved organic matter: Impacts of aromaticity and carbonyl groups, *Sci. Total Environ.*, 2023, **871**, 162048.
57 F. Yang, Q. Zhang, H. X. Jian, C. P. Wang, B. S. Xing, H. W. Sun and Y. L. Hao, Effect of biochar-derived dissolved organic matter on adsorption of sulfamethoxazole and chloramphenicol, *J. Hazard. Mater.*, 2020, **396**, 122598.
58 B. B. Xu, J. H. Li, Q. H. Huang, Q. W. Gong and L. H. Li, Impacts of land use patterns and typhoon-induced heavy rainfall event on dissolved organic matter properties in the South Tiaoxi River, China, *Environ. Earth Sci.*, 2016, **75**, 632.
59 J. Y. Chen, H. Y. Zhang, Q. Q. Wei, U. Farooq, Q. Zhang, T. T. Lu, X. H. Wang, W. F. Chen and Z. C. Qi, Mobility of water-soluble aerosol organic matters (WSAOMs) and their effects on soil colloid-mediated transport of heavy metal ions in saturated porous media, *J. Hazard. Mater.*, 2022, **440**, 129733.
60 S. Miao, H. Lyu, J. Xu, S. Bi, H. L. Guo, M. Mu, S. H. Lei, S. Zeng and H. Q. Liu, Characteristics of the chromophoric dissolved organic matter of urban black-odor rivers using fluorescence and UV-visible spectroscopy, *Environ. Pollut.*, 2021, **268**, 115763.
61 J. Y. Chen, H. Y. Zhang, U. Farooq, Q. Zhang, J. Z. Ni, R. H. Miao, W. F. Chen and Z. C. Qi, Transport of dissolved organic matters derived from biomass-pyrogenic smoke (SDOMs) and their effects on mobility of heavy metal ions in saturated porous media, *Chemosphere*, 2023, **336**, 139247.
62 L. Wu, J. Z. Ni, H. Y. Zhang, S. H. Yu, R. Wei, W. Qian, W. F. Chen and Z. C. Qi, The composition, energy, and carbon stability characteristics of biochars derived from thermo-conversion of biomass in air-limitation, CO_2, and N_2 at different temperatures, *Waste Manage.*, 2022, **141**, 136–146.
63 J. Xing, G. R. Xu and G. B. Li, Analysis of the complexation behaviors of Cu(II) with DOM from sludge-based biochars and agricultural soil: Effect of pyrolysis temperature, *Chemosphere*, 2020, **250**, 126184.
64 X. J. Jiang, M. P. Tong and H. Kim, Influence of natural organic matter on the transport and deposition of zinc oxide nanoparticles in saturated porous media, *J. Colloid Interface Sci.*, 2012, **386**, 34–43.
65 C. H. Miao, H. Zhou, Y. Z. Lv, J. Y. Shang and A. Mamut, Combined effects of ferrihydrite coating and ionic type on the transport of compost-derived dissolved organic matter in saturated porous media, *Environ. Pollut.*, 2022, **307**, 119501.
66 Q. Q. Wei, K. Zhou, J. Y. Chen, Q. Zhang, T. T. Lu, U. Farooq, W. F. Chen, D. L. Li and Z. C. Qi, Insights into the molecular mechanism of tetracycline transport in saturated porous media affected by low-molecular-weight organic acids: Role of the functional groups and molecular size, *Sci. Total Environ.*, 2021, **799**, 149361.
67 Y. H. Jin, J. Y. Chen, Q. Zhang, U. Farooq, T. T. Lu, B. Wang, Z. C. Qi and W. F. Chen, Biosurfactant-affected mobility of oxytetracycline and its variations with surface chemical heterogeneity in saturated porous media, *Water Res.*, 2023, **244**, 120509.
68 X. Y. Qian, J. Ma, L. P. Weng, Y. L. Chen, Z. L. Ren and Y. T. Li, Influence of agricultural organic inputs and their aging on the transport of ferrihydrite nanoparticles: From enhancement to inhibition, *Sci. Total Environ.*, 2020, **719**, 137440.
69 H. X. Xu, H. Tian, J. S. Deng, Q. M. Zhuo, J. H. Cui, J. Z. Wang, Y. A. Yin and P. Yu, Review of influence of steric effect on aggregation behavior of fine particles, *Miner. Eng.*, 2023, **203**, 108304.
70 R. C. Zhang, C. Tu, H. B. Zhang and Y. M. Luo, Enhancing effects of dissolved and media surface-bound organic matter on titanium dioxide nanoparticles transport in iron oxide-coated porous media under acidic conditions, *J. Hazard. Mater.*, 2022, **438**, 129421.
71 J. Giammarco, V. N. Mochalin, J. Haeckel and Y. Gogotsi, The adsorption of tetracycline and vancomycin onto nanodiamond with controlled release, *J. Colloid Interface Sci.*, 2016, **468**, 253–261.
72 J. Li, H. Zhang and G. D. Yuan, Phosphate affects adsorption and desorption of oxytetracycline in the seawater-sediment systems, *Environ. Sci. Pollut. Res.*, 2018, **25**, 28160–28168.
73 S. N. Dong, B. Gao, Y. Y. Sun, X. Q. Shi, H. X. Xu, J. F. Wu and J. C. Wu, Transport of sulfacetamide and levofloxacin in granular porous media under various conditions: Experimental observations and model simulations, *Sci. Total Environ.*, 2016, **573**, 1630–1637.

74 D. Durce, M. Aertsens, D. Jacques, N. Maes and M. Van Gompel, Transport of dissolved organic matter in Boom Clay: Size effects, *J. Contam. Hydrol.*, 2018, **208**, 27–34.
75 J. F. Mccarthy, L. Liang, P. M. Jardine, D. L. Taylor and L. W. Jolley, Mobility of natural organic matter in a sandy aquifer, *Environ. Sci. Technol.*, 1993, **27**, 667–676.
76 J. J. Xu, J. F. Niu, X. Q. Zhang, J. Liu, G. P. Cao and X. R. Kong, Sorption of triclosan on electrospun fibrous membranes: Effects of pH and dissolved organic matter, *Emerging Contam.*, 2015, **1**, 25–32.
77 X. T. Zhao, Z. Z. Hu, X. Yang, X. W. Cai, Z. W. Wang and X. Y. Xie, Noncovalent interactions between fluoroquinolone antibiotics with dissolved organic matter: A 1H NMR binding site study and multi-spectroscopic methods, *Environ. Pollut.*, 2019, **248**, 815–822.
78 J. Jin and A. R. Zimmerman, Abiotic interactions of natural dissolved organic matter and carbonate aquifer rock, *Appl. Geochem.*, 2010, **25**, 472–484.
79 D. I. Kreller, Y. Wu, S. Sutton and A. Furio, Adsorption and Fractionation of Suwannee River Organic Matter on Metal (Fe, Al) Oxide-Coated Quartz: A Liquid Chromatographic Investigation, *Environ. Eng. Sci.*, 2015, **32**, 45–53.
80 M. Paradelo, P. Perez-Rodriguez, D. Fernandez-Calvino, M. Arias-Estevez and J. E. Lopez-Periago, Coupled transport of humic acids and copper through saturated porous media, *Eur. J. Soil Sci.*, 2012, **63**, 708–716.
81 H. Chen, B. Gao, H. Li and L. Q. Ma, Effects of pH and ionic strength on sulfamethoxazole and ciprofloxacin transport in saturated porous media, *J. Contam. Hydrol.*, 2011, **126**, 29–36.
82 V. Artifon, E. Zanardi-Lamardo and G. Fillmann, Aquatic organic matter: Classification and interaction with organic microcontaminants, *Sci. Total Environ.*, 2019, **649**, 1620–1635.
83 Y. Yamashita, T. Tanaka and Y. Adachi, Transport behavior and deposition kinetics of humic acid under acidic conditions in porous media, *Colloids Surf., A*, 2013, **417**, 230–235.
84 M. J. Wang, Q. Zhang, T. T. Lu, J. Y. Chen, Q. Q. Wei, W. F. Chen, Y. M. Zhou and Z. C. Qi, Colloid-mediated transport of tetracycline in saturated porous media: Comparison between ferrihydrite and montmorillonite, *J. Environ. Manage.*, 2021, **299**, 113638.
85 R. A. Figueroa and A. A. Mackay, Sorption of oxytetracycline to iron oxides and iron oxide-rich soils, *Environ. Sci. Technol.*, 2005, **39**, 6664–6671.
86 J. Y. Park and B. Huwe, Effect of pH and soil structure on transport of sulfonamide antibiotics in agricultural soils, *Environ. Pollut.*, 2016, **213**, 561–570.
87 J. D. Lanphere, B. Rogers, C. Luth, C. H. Bolster and S. L. Walker, Stability and Transport of Graphene Oxide Nanoparticles in Groundwater and Surface Water, *Environ. Eng. Sci.*, 2014, **31**, 350–359.
88 W. W. Li, H. J. Zhang, T. T. Lu, Y. X. Li, Y. M. Song, Z. B. Shang, S. H. Liu, D. L. Li and Z. C. Qi, Effects of divalent metal cations and inorganic anions on the transport of tetracycline in saturated porous media: column experiments and numerical simulations, *Environ. Sci.: Processes Impacts*, 2019, **21**, 1153–1163.
89 M. Y. Jia, F. Wang, Y. R. Bian, X. Jin, Y. Song, F. O. Kengara, R. K. Xu and X. Jiang, Effects of pH and metal ions on oxytetracycline sorption to maize-straw-derived biochar, *Bioresour. Technol.*, 2013, **136**, 87–93.
90 R. A. Figueroa-Diva, D. Vasudevan and A. A. MacKay, Trends in soil sorption coefficients within common antimicrobial families, *Chemosphere*, 2010, **79**, 786–793.
91 M. Pan, Biochar Adsorption of Antibiotics and its Implications to Remediation of Contaminated Soil, *Water, Air, Soil Pollut.*, 2020, **231**, 221.
92 M. A. Ghandour, H. A. Azab, A. Hassan and A. M. Ali, Voltammetric studies on composition and stabilities of complexes of tetracycline and oxytetracycline with some metal ions in aqueous medium, *Monatsh. Chem.*, 1992, **123**, 853–864.
93 W. D. Kong, C. G. Li, J. M. Dolhi, S. Y. Li, J. Z. He and M. Qiao, Characteristics of oxytetracycline sorption and potential bioavailability in soils with various physical-chemical properties, *Chemosphere*, 2012, **87**, 542–548.
94 B. Gunawardana, N. Singhal and A. Johnson, Effects of Amendments on Copper, Cadmium, and Lead Phytoextraction by Lolium Perenne from Multiple-Metal Contaminated Solution, *Int. J. Phytorem.*, 2011, **13**, 215–232.
95 H. Murano, K. Suzuki, S. Kayada, M. Saito, N. Yuge, T. Arishiro, A. Watanabe and T. Isoi, Influence of humic substances and iron and aluminum ions on the sorption of acetamiprid to an arable soil, *Sci. Total Environ.*, 2018, **615**, 1478–1784.
96 Y. Y. Tan, Y. Guo, X. Y. Gu and C. Gu, Effects of metal cations and fulvic acid on the adsorption of ciprofloxacin onto goethite, *Environ. Sci. Pollut. Res.*, 2015, **22**, 609–617.

